ELSEVIER

Journal of Biomechanics 34 (2001) 1145–1155

JOURNAL OF BIOMECHANICS

www.elsevier.com/locate/jbiomech
www.JBiomech.com

# Determination of wave speed and wave separation in the arteries

A.W. Khir[a,*], A. O'Brien[a], J.S.R. Gibbs[b], K.H. Parker[a]

[a] *Physiological Flow Studies Group, Department of Biological and Medical Systems, Imperial College of Science, Technology and Medicine London, SW7 2AZ, UK*

[b] *Department of Cardiology, National Heart and Lung Institute, Imperial College of Science, Technology and Medicine London, SW7 2AZ, UK*

Accepted 11 April 2001

**Abstract**

Considering waves in the arteries as infinitesimal wave fronts rather than sinusoidal wavetrains, the change in pressure across the wave front, $dP$, is related to the change in velocity, $dU$, that it induces by the 'water hammer' equation, $dP = \pm \rho c\, dU$, where $\rho$ is the density of blood and $c$ is the local wave speed. When only unidirectional waves are present, this relationship corresponds to a straight line when $P$ is plotted against $U$ with slope $\rho c$. When both forward and backward waves are present, the $PU$-loop is no longer linear. Measurements in latex tubes and systemic and pulmonary arteries exhibit a linear range during early systole and this provides a way of determining the local wave speed from the slope of the linear portion of the loop. Once the wave speed is known, it is also possible to separate the measured $P$ and $U$ into their forward and backward components. In cases where reflected waves are prominent, this separation of waves can help clarify the pattern of waves in the arteries throughout the cardiac cycle. 

## 1. Introduction

The wave nature of pressure and flow in the arteries has long been recognised (Young, 1809). Recognition of the influence of wave reflections came much later but it is now generally accepted that '*There is in fact no circumstance in life where pressure and flow are not altered by wave reflection*; *this is a consequence of the varying properties of the vascular bed along its length*, *its branching pattern, and particularly the steep rise in fluid resistance within the muscular arterioles*'. (Nichols and O'Rourke, 1990). The first technique for separating measured pressure and flow waveforms into their forward and backward components is based upon the impedance analysis and the assumption that the higher harmonics of the waveform will be dissipated so quickly that the higher harmonics of the reflected wavetrains will be negligible compared to those in the forward wavetrains (Westerhof et al., 1972). The ratio of pressure to flow for these higher harmonics is called the *characteristic impedance*, $Z_0 = \bar{P}_+/\bar{U}_+ = -\bar{P}_-/\bar{U}_-$, where $\bar{P}$ is magnitude of the sinusoidal pressure, $\bar{U}$ is magnitude of the average velocity and subscripts '+' and '−' refer to forward and backward waves.

Parker and Jones (1990) suggested an alternative method of separating forward and backward waves based upon the method of characteristics solution of the one-dimensional conservation equations for flow in the arteries. This analysis, which forms the basis of the current work, is based upon a non-linear analysis and considers the propagation of incremental wave fronts rather than sinusoidal wave trains. It includes the effects of convection of the waves and the possibility that the wave speed can vary with instantaneous pressure but assumes that the forward and backward waves sum linearly when they interact. This assumption was relaxed by Pythoud et al. (1996), who considered the full non-linear analysis. Their work concludes that the differences between the fully non-linear and the linearised analyses are small. We believe that in most cases they do not warrant the considerable extra work involved in the numerical inversion of integral equations which their method requires.

Both the impedance method and the method discussed here for wave separation require knowledge of the wave speed, the speed at which disturbances will propagate in the elastic vessel in the absence of any

*Corresponding author.

0021-9290/01/$ - see front matter 
PII: S0021-9290(01)00076-8

convective velocity. Many methods for determining wave speed in arteries have been proposed (Milnor, 1989). Many of these measurements are based upon simultaneous measurements of pressure or flow at two sites in the arteries and the determination of the time it takes a wave to propagate from one site to the other. By their nature, these measurements can only indicate the average wave speed over the distance between the measurement sites and, because the properties of arteries can vary significantly throughout the arterial tree, this can be a serious shortcoming. For this reason we believe that methods which determine the local wave speed from the simultaneous measurement of pressure and velocity at the same site are preferable. Herein we present such a method and discuss its application to experimental data.

Given knowledge of the local wave speed, measured pressure and velocity waveforms can be separated into their forward and backward components. We will present a method based upon the calculation of wave intensity which derives from the general solution of the one-dimensional conservation equations in the arteries (Parker and Jones, 1990). This theory can be developed for very general conditions but, for ease of presentation, we will neglect both viscous losses and fluid transport out of the arteries. These effects can be included in the analysis without affecting the wave nature of the solution. However, because their effects are relatively small and because including them would require more detailed information about local haemodynamics than is available experimentally, we omit them here.

## 2. Theoretical background

The theoretical basis of this work is the solution of the one-dimensional equations for flow in an elastic artery using the method of characteristics (Parker and Jones, 1990). This analysis is somewhat complex but the results are surprisingly simple: Disturbances to the flow create changes in pressure, $P$, and velocity, $U$, which propagate downstream (forward) with speed $U+c$ and upstream (backward) with speed $U-c$, where $c$ is the wave speed. Furthermore, the wavespeed, $c=1/\sqrt{\rho D}$, is simply a function of the density of the blood $\rho$ and the distensibility of the artery, $D=(1/A)\,\mathrm{d}A/\mathrm{d}P$, where $A$ is the cross sectional area of the artery.

From the conservation of mass and momentum, there is a simple relationship between the changes in pressure and velocity across any of these wavefronts given by the 'water hammer' equation

$$\mathrm{d}P_{\pm} = \pm\rho c\,\mathrm{d}U_{\pm}, \tag{1}$$

where $\rho$ is the density of the blood and the '+' sign refers to forward travelling waves and the '−' sign refers to backward waves. If the forward and backward waves are additive, i.e.

$$\mathrm{d}P = \mathrm{d}P_{+} + \mathrm{d}P_{-}, \tag{2}$$

$$\mathrm{d}U = \mathrm{d}U_{+} + \mathrm{d}U_{-}, \tag{3}$$

then it is possible to calculate the forward and backward waves (incremental wave fronts) from the measured $\mathrm{d}P$ and $\mathrm{d}U$.

$$\mathrm{d}P_{\pm} = \tfrac{1}{2}(\mathrm{d}P \pm \rho c\,\mathrm{d}U), \tag{4}$$

$$\mathrm{d}U_{\pm} = \pm\tfrac{1}{2}(\mathrm{d}P/\rho c \pm \mathrm{d}U). \tag{5}$$

Once we have calculated the changes in pressure and velocity in the forward and backward waves, the forward and backward pressure waveform can be calculated by simply summing the instantaneous differences

$$P_{+} = P_{\mathrm{d}} + \sum_{t=0}^{t} \mathrm{d}P_{+}, \quad P_{-} = \sum_{t=0}^{t} \mathrm{d}P_{-}, \tag{6}$$

$$U_{+} = \sum_{t=0}^{t} \mathrm{d}U_{+}, \quad U_{-} = \sum_{t=0}^{t} \mathrm{d}U_{-}, \tag{7}$$

where the integration constant, $P_{\mathrm{d}}$, is taken to be the diastolic pressure (defined as the minimum pressure during the cardiac cycle) which is ascribed, arbitrarily, to the forward pressure wave. The integration constant for $U$ is taken to be zero.

When considering forward and backward waves, it is often convenient to define the wave intensity $\mathrm{d}I = \mathrm{d}P\,\mathrm{d}U$, which represents the flux of energy carried by the wave. Waves are generally classified by the sign of the change in pressure that they produce, compression waves have $\mathrm{d}P>0$ and expansion waves have $\mathrm{d}P<0$. From the water hammer equation we see that forward compression waves cause acceleration of the blood, $\mathrm{d}U>0$, while forward expansion waves cause deceleration, $\mathrm{d}U<0$. To the contrary, backward compression waves cause deceleration of the blood while backward expansion waves cause acceleration. This somewhat confusing state of affairs is simplified if we consider the wave intensity because the wave intensity of all forward waves is positive, $\mathrm{d}I_{+} = \mathrm{d}P_{+}\mathrm{d}U_{+} > 0$ and of all backward waves is negative, $\mathrm{d}I_{-} = \mathrm{d}P_{-}\mathrm{d}U_{-} < 0$. Furthermore, the measured wave intensity at every instant is the sum of the wave intensities of the forward and backward waves, $\mathrm{d}I = \mathrm{d}I_{+} + \mathrm{d}I_{-}$, and thus reflects the net importance of forward and backward waves at each instant in the cardiac cycle.

From the above, it is apparent that it is necessary to know the wave speed before the measured pressure and velocity waveforms can be separated into their forward and backward components. Fortunately, the theory also suggests a way of determining the local wave speed. During the periods when there are no backward waves, e.g. at the start of systole, the water hammer equation (1) indicates that there should be a linear relationship

between the change in pressure and the change in velocity. Thus, if we plot $P$ vs. $U$ over a cardiac cycle, a $PU$-loop, the part of the loop corresponding to early systole should be linear with slope equal to $\rho c$. Developing this method for determining the wavespeed is one of the principal objectives of this paper.

For the results presented here, the slope of the linear portion of the $PU$-loop was determined by fitting a straight line to the appropriate part of the data by eye using a mouse driven graphical interface on the computer. An alternative would be to select the portion of the data to be analysed and then determine the best fit line by linear regression. While this procedure does provide a quantitative measure of the goodness of fit, it is also dependent upon the choice of the segment of data to be analysed which is also subjective. Comparison of results obtained from the same data by independent analysts using the interactive computer program showed that the results always differed by less than 5%. As will be demonstrated below, this difference in the wave speed has a negligible effect on the results for the separation of waves into the forward and backward components and we therefore opted for this simpler procedure for determining the slope and hence the wave speed.

The assumption that there is a period in early systole when there are no reflected waves also provides us with a means of determining the simultaneity of the measured pressure and velocity waveforms. This can be important practically because most methods of measuring velocity or flow rate involve some delay in the transducer output, either low-pass filters in electromagnetic flow meters or processing algorithms in Doppler ultrasound devices. By shifting the velocity waveform in increments of the sampling frequency and plotting the $PU$-loop, it is generally very easy to determine the time shift which produces the best straight line relationship during early systole.

Having determined the wavespeed, we use the equations above to determine the forward and backward waves from the simultaneously measured pressure and velocity. In the systemic arteries, the forward waves are mainly generated by the heart and the backward waves arise from reflections from the periphery and therefore the calculation of the separated waves can aid in the interpretation of the physiology and pathology of the cardiovascular system.

## 3. Results

### 3.1. Determination of the wave speed

Fig. 1 shows the pressure and velocity waveforms and the corresponding $PU$-loop measured at the proximal end of a latex tube in response to an approximately half sinusoidal injection of fluid from a syringe pump (Khir,

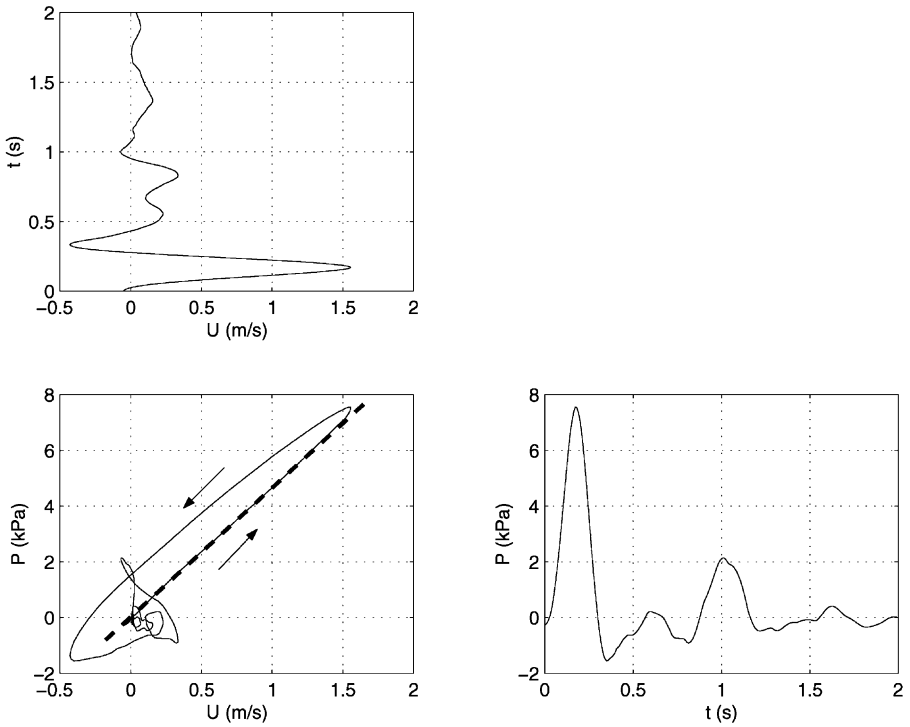


Fig. 1. $P(t)$, $U(t)$ and the $PU$-loop measured in a latex tube in response to a half sinusoidal injection of fluid from a syringe pump at the upstream end of the tube.

1999). The tube was 110 cm long and 1.3 cm in diameter and it was connected at the distal end to a constant height reservoir. The slope of the *PU*-loop is very linear from the start of the injection to the point of peak velocity and the slope corresponds to a wave speed of 4.5 m/s assuming a density of 9% saline of 1080 kg/m$^3$. From this measured wave speed and the distance from the point of measurement to the distal reservoir and back again, we would expect a reflected wave to arrive at the measurement site 0.5 s from the start of the injected waveform. Indeed, we see that the $P$ and $U$ waveforms do begin to deviate significantly from each other after this time interval.

The *PU*-loops from data measured by a catheter mounted strain gauge and a cuff ultrasonic flow meter in the ascending aorta of an anaesthetised dog under control conditions are shown in the bottom part of Fig. 2(a) (Khir, 1999). Because time becomes a parameter of the curves and is not apparent, we plot $P$ as a function of $t$ with a common axis in Fig. 2(b). Note, in particular, the linear portion of the *PU*-loop corresponding to the initial portion of systole. The linearity of this part of the curve indicates that only forward waves are present and the slope of the straight line corresponds to $\rho c$. The indicated slope corresponds to $c = 6.2$ m/s, taking the density of blood to be 1040 kg/m$^3$. Also note that the *PU*-loop deviates from the linear at $P \simeq 15$ KPa and that the time of this deviation indicates the time of arrival of the first of the reflected waves.

Also shown in the upper half of Fig. 2(a) and (b) are data measured in the same dog when the upper thoracic aorta was occluded 14.5 cm from the measurement site in the ascending aorta. We see first that the mean pressure is greatly increased during occlusion of the aorta. Secondly, the part of the *PU*-loop corresponding to the start of systole is still linear with a slope corresponding to $c = 7.9$ m/s, significantly larger than that determined before occlusion as would be expected from the higher mean pressure. Finally, we note that the linear part of the curve deviates from the linear much sooner because of the early arrival of a backward, reflected wave from the site of occlusion. Again the time over which the *PU*-loop is linear corresponds well to the time of travel of the wave with the measured wave speed over the measured distance to the site of occlusion, 37 ms, or approximately seven sample points.

Finally, Fig. 3 shows a *PU*-loop measured with a catheter mounted strain gauge and Doppler ultrasound velocity transducer in the main pulmonary artery of a patient undergoing catheterisation for coronary artery disease. Once again, we note that there is a distinct linear portion of the curve during early systole. In this case, the slope corresponds to a wave speed of 5.1 m/s.

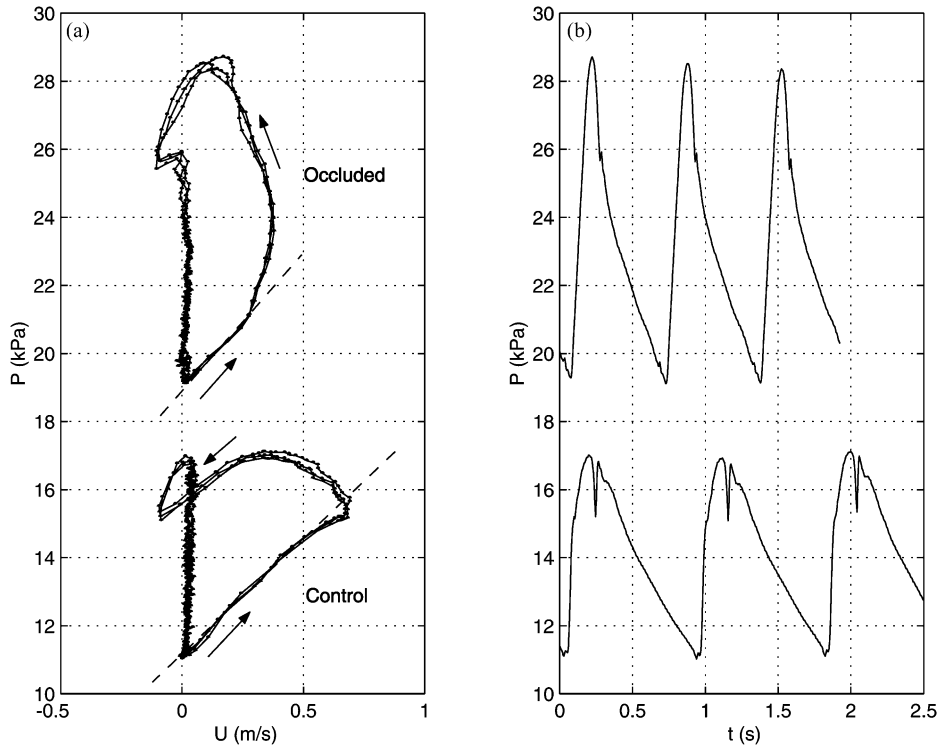


Fig. 2. (a) The *PU*-loop, the dots correspond to the data sampled at 200 Hz and (b) $P(t)$ measured in the ascending aorta of the dog under control conditions (lower curves) and with total occlusion of the upper thoracic aorta (upper curves). The dashed lines indicates the slope of the linear portion of the curve during early systole.

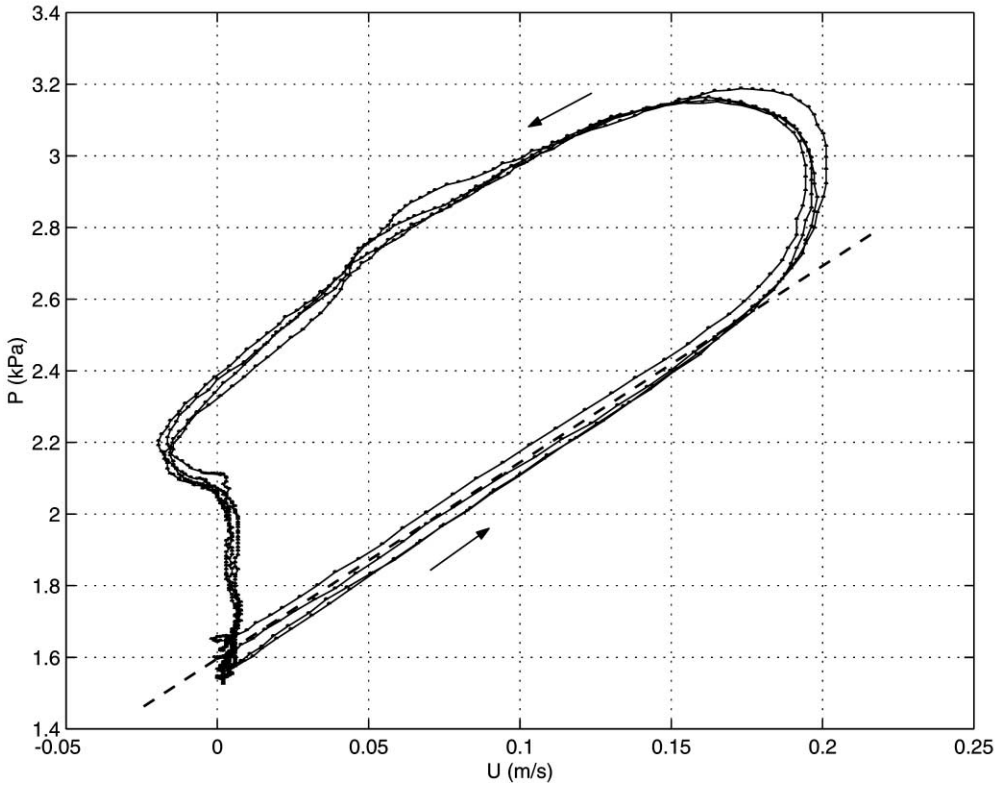


Fig. 3. The $PU$-loop measured in the human main pulmonary artery. The dashed line indicates the slope of the linear portion of the curve during early systole.

### 3.2. Determination of time lags

Fig. 4 shows the effect of a time lag on the $PU$-loop. The central loop corresponds to the $P$ and $U$ data adjusted to correct for the time lag of the velocity transducer determined by calibration prior to the experiment. The other curves correspond to $U$ leading and lagging $P$ by 1 and 2 sampling intervals. If the velocity lags the pressure too much, the initial slope approaches $\infty$ and if the pressure lags the velocity the initial slope approaches zero. As the lag is changed from one extreme to the other, the initial portion of the curve goes from concave to linear to convex as illustrated in Fig. 4. In cases where transducer calibrations are unavailable, we have found this to be a robust and repeatable method of determining the appropriate time lag between the pressure and velocity measurements.

### 3.3. Separation of forward and backward waves

Fig. 5 shows the pressure and velocity measured in the ascending aorta of an anaesthetised dog under control conditions for a period including three cardiac cycles (the same data used in Fig. 2). Below these measurements is the wave intensity $dI$ calculated for these data. Three characteristics of the wave intensity waveform should be noted:

(a) The positive peak occurring at the start of systole represents the initial, forward compression ($dP > 0$) wave generated by the contraction of the ventricle.

(b) The second positive peak occurring at the end of systole indicates that there is a forward expansion ($dP < 0$) wave dominating the flow at this time of the cardiac cycle. This indicates that it is a forward wave generated by the inability of the ventricle to contract quickly enough to keep up with the momentum of the blood in the arteries generated by the earlier part of systole that is the predominant cause of the stopping of blood flow at the end of systole (Parker et al., 1988).

(c) In mid-systole there is a period when the wave intensity is negative, indicating that backward, reflected waves are dominating the forward waves.

Fig. 6(a) shows the net wave intensity $dI$ and the separated wave intensities $dI_{\pm}$ for the data shown in Fig. 5 and the lower part of Fig. 2. The net wave intensity is the algebraic sum of a positive forward wave intensity and a negative backward wave intensity and, because there is little overlap of the forward and backward waves, most of the information about the waves can be inferred from the net wave intensity alone.

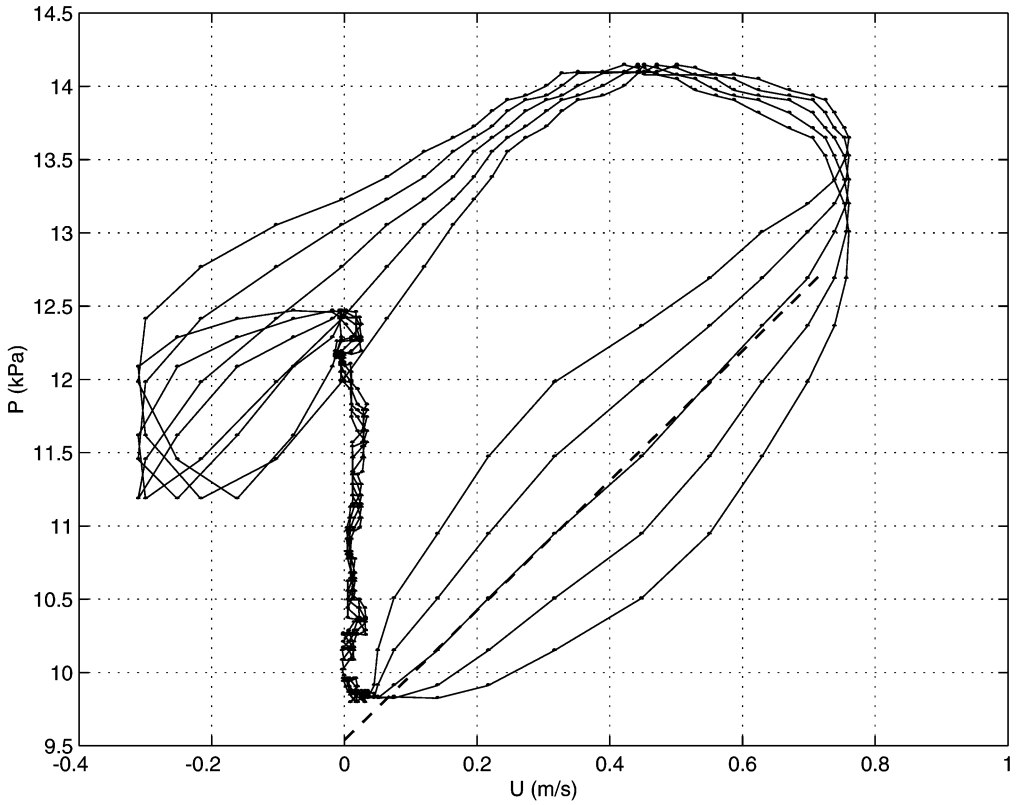


Fig. 4. The $PU$-loop for different time lags between $P$ and $U$. The centre loop represents the optimal condition, no time lag, as judged by the linearity of the portion of the loop corresponding to early systole indicated by the dashed line. The two curves above and below the optimal loop correspond to $U$ lagging and leading $P$ by 1 and 2 sampling intervals.

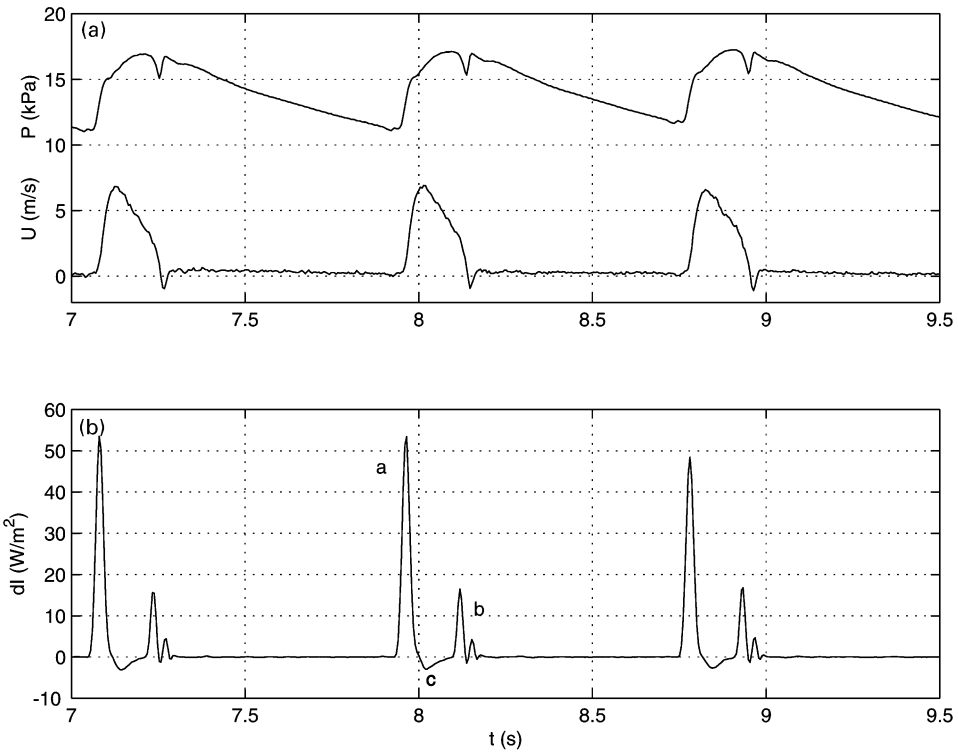


Fig. 5. (a) $P(t)$ and $U(t)$ measured in the ascending aorta of the dog under control conditions. (b) d$I$ calculated from the data in (a); a—the initial, forward compression wave at the start of systole, b—forward expansion wave at the end of systole, c—backward, reflected waves in mid-systole.

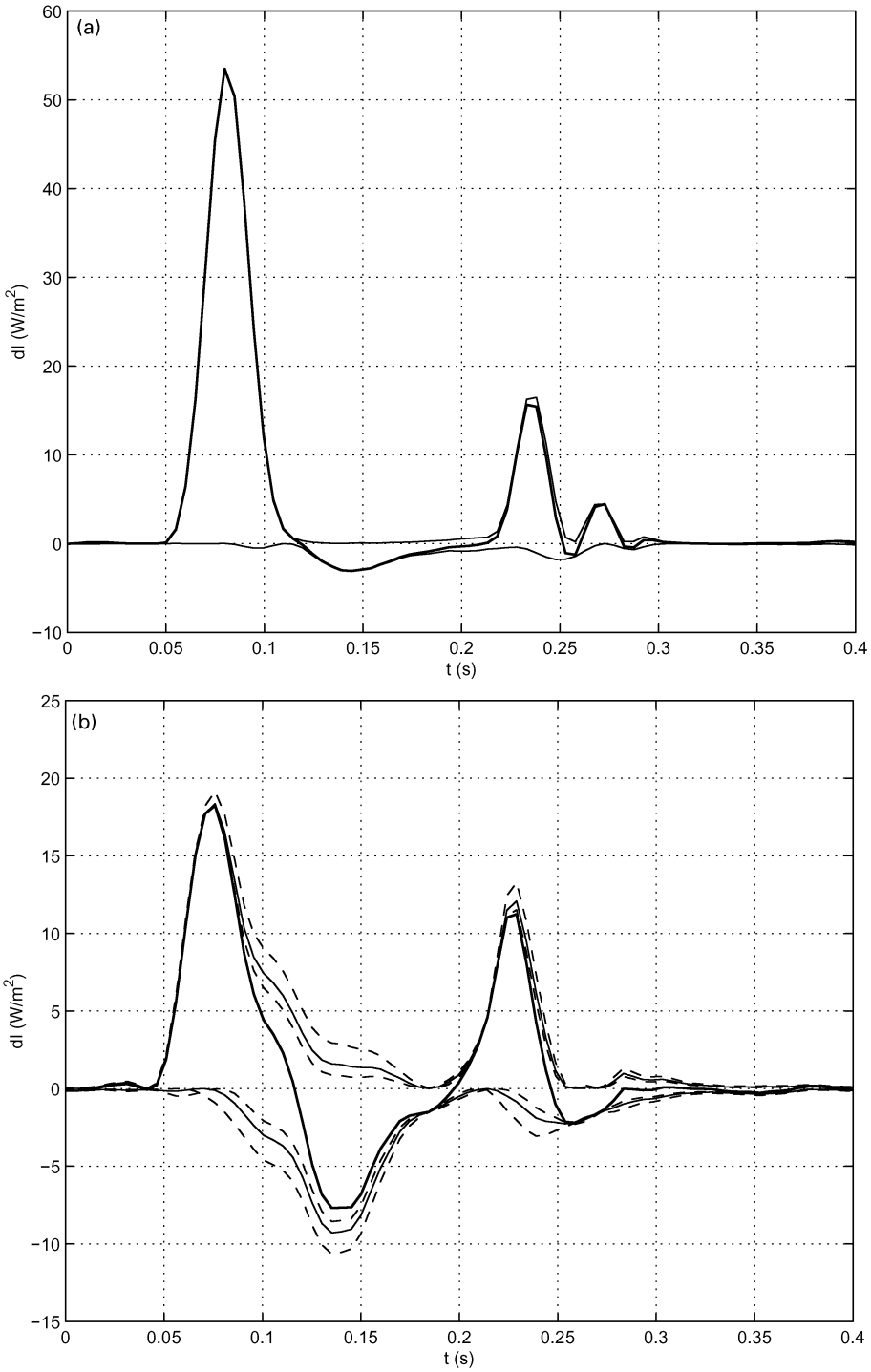


Fig. 6. d$I$ and d$I_{\pm}$ calculated for data measured in the ascending aorta of the dog (a) under control conditions and (b) with a total occlusion of the upper thoracic aorta. Note the different scales of the ordinate. d$I_{+}$ is always positive, d$I_{-}$ is always negative and the darker line, d$I$, is the sum of the two. In (b) the dashed lines indicate d$I_{+}$ and d$I_{-}$ calculated for values of $c \pm 20\%$.

This is not the case when the aorta is occluded as for the data shown in the top half of Fig. 2. The net wave intensity d$I$ and the separated wave intensities d$I_{\pm}$ for these data are shown in Fig. 6(b). In this case, the reflected wave arrives in the ascending aorta well before the end of the initial forward compression wave, information that cannot be inferred from the net wave intensity alone. The dashed lines in Fig. 6(b) correspond to the forward and backward wave intensities calculated for a wave speed 20% larger and smaller than the wave speed determined from the $PU$-loop. Whenever it has been possible in our experiments to compare $PU$-loop

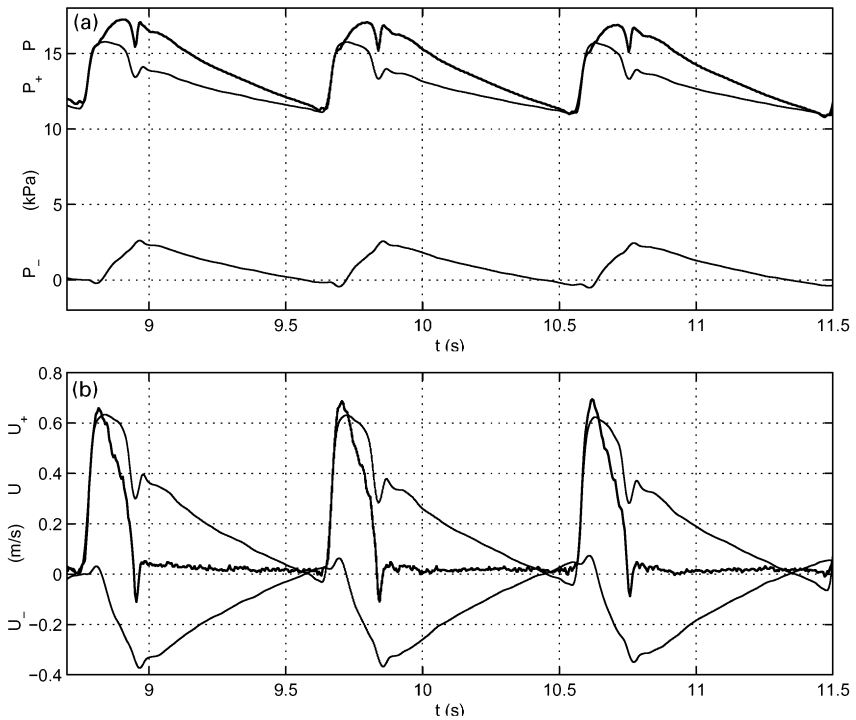


Fig. 7. (a) The measured pressure, $P(t)$, and the separated forward and backward pressure waveforms, $P_{\pm}(t)$ (b) The measured velocity, $U(t)$, and the separated forward and backward velocity waveforms, $U_{\pm}(t)$, measured in the ascending aorta of the dog under control conditions.

results with foot-to-foot measurements, the differences have always been much less than 20%. This shows that the sensitivity of the separation process is not highly dependent upon the accuracy of the determination of the wave speed.

The separated pressure and velocity waveforms, $P_{\pm}$ and $U_{\pm}$, calculated from the data measured in the ascending aorta under control conditions are shown in Fig. 7. The waveform of the backward wave, $P_{-}$ and $U_{-}$, indicate that the reflected waves are initially compression waves, $\mathrm{d}P_{-} > 0$ and $\mathrm{d}U_{-} < 0$, followed by expansion waves during the latter parts of the cardiac cycle. Since this is the same as the pattern of the forward waveform, this indicates that the wave reflections are predominantly positive.

## 4. Conclusions and discussion

Previous discussions of wave speed and the separation of waves into their forward and backward components in the arteries have been expressed almost exclusively in terms of the sinusoidal wavetrains which are the basis of impedance analyses (Westerhof et al., 1972; Milnor, 1989; Nichols and O'Rourke, 1990). In the absence of reflections, the ratio of the pressure and the velocity waveforms, the characteristic impedance, is $Z_c = \bar{P}/\bar{U} = \rho c$ where $\bar{P}$ is the magnitude of a sinusoidal pressure pulse and $\bar{U}$ is the magnitude of the accompanying sinusoidal average velocity, which is consistent with the waterhammer equation for sinusoidal waveforms.

The major difference between the two approaches is in the identification of the conditions under which reflections are not important. In the method proposed here, this is done simply by determining the period during early systole when there is a linear relationship between P and U. In the frequency-based impedance analysis it is usually argued that the increasing dissipation with increasing frequency makes it likely that reflected waves will be less important for the higher harmonics. Since noise also increases with increasing frequency, the characteristic frequency is generally taken as the average impedance calculated for a range of frequencies or harmonics. The choice is somewhat subjective and its effect on the determination of the characteristic impedance, and therefore the wave speed, has been studied by Dujardin and Stone (1981). Analysing data from 10 dogs using the averaging algorithms suggested by different authors to calculate $Z_c$, their plotted results show a range of values varying at least 20% from the middle of the range (Belinda et al., 1994). This range of variation of the characteristic impedance depending upon the averaging algorithm is consistent with our experience and makes a definitive comparison of methods difficult.

Interestingly, Dujardin and Stone (1981) also described a time-based method for determining wave

speed. Arguing that the early upstroke of the pressure and flow curves during early ejection should be governed by the high-frequency components of the input impedance spectrum and therefore $\Delta P/\Delta U$ at the time of maximum $dP/dt$ and $dU/dt$ should be comparable to the characteristic impedance. Apart from the theoretical justification and the use of $U$–$P$ loops, this method is essentially the same as that proposed in this paper. Li (1986) also used the characteristic impedance relationship to suggest that $\Delta P/\Delta U$ during the rapid rise could be used to determine $c$ although there is no discussion of how to determine the period over which $\Delta P$ and $\Delta U$ should be taken.

Other methods which have been used to determine the wave speed involve measuring the time that it takes a wave to travel over a measured distance along the artery. The wave can be measured from simultaneous pressures (Latham et al., 1985) or velocities measured by Doppler ultrasound (Avolio et al., 1983). Apart from the difficulties of making simultaneous measurements at two different sites and the difficulty in measuring the distance accurately, these methods can, at best, provide an average wave speed over the distance between the two sites of measurement. More recently, magnetic resonance methods of measuring wave speed have been proposed that overcome some of these problems (Dumoulin et al., 1993) but their accuracy has yet to be established.

We carried out a number of experiments with latex tubing to ascertain the accuracy of this method of determining the wave speed. In these experiments we measured $P$ and $U$ at the upstream end of the tube and $P$ at the downstream end so that we could compare wave speed determined using the $PU$-loop with that determined from the foot-to-foot delay time between the upstream and downstream measurements of $P$ (Khir, 1999). In general, the agreement between the two measurements of wave speed was excellent, differing at most by 5%. Both methods presented minor difficulties in the determination of wave speed. The $PU$-loop method is sensitive to the choice of the portion of the curve to be analysed by linear regression for the slope. The foot-to-foot method is similarly sensitive to the method used to determine the foot of the waveforms. Analysis of the error sensitivities of the two methods suggested that neither is inherently more accurate than the other and that the relatively small differences between the two methods of measurement cannot be resolved.

The application of the $PU$-loop method of determining wave speed from measurements in arteries seems very promising. In normal conditions in both the ascending aorta (Fig. 2) and the main pulmonary artery (Fig. 3) there is a very distinct linear portion of the curve corresponding to early systole. From our experience with other data from these experiments and from others not described, we find that this linear portion is a regular and easily identifiable feature of $PU$-loops. Once the linear portion is identified, the slope is easily obtained, either by eye or by linear regression, and wave speed follows simply by dividing by the density of blood. One indication of the robustness of the method is seen in both Figs. 2 and 3 where three successive cardiac cycles are plotted giving a good indication of the beat by beat variation of the loops.

Fig. 2 also shows the method being applied to two very different conditions, control conditions and during complete occlusion of the upper thoracic aorta. We see that under control conditions (the lower curves) the linear portion of the $PU$-loop extends over approximately the first two thirds of the pressure rise in early systole. The deviation of the curve from the linear is fairly gentle and, in this particular case, concave towards the $U$ axis. This means that the reflected waves first arrive at the ascending aorta at this time and are relatively small. It also means that these first reflected waves are expansion waves ($dP_- < 0$) which, incidentally, is not always the case.

When the aorta is occluded (the upper curves) the linear portion of the $PU$-loop is much shorter, corresponding to less than the first quarter of the pressure rise during early systole. The curve deviates from the linear very sharply and in the direction of increasing pressure, indicating that a large reflected compression wave ($dP_- > 0$) has arrived, just as would be expected when the descending aorta is occluded. Even though the time when only forward waves are present is short, it is still easy to find the slope of the linear part of the $PU$-curve and determine the wave speed from it. As can be seen in Fig. 2, the slope and therefore the wave speed is higher during clamping of the aorta. Since arteries are generally less distensible at increased pressure, this increase in wave speed is expected due to higher mean pressure during aortic clamping.

The wave speed determined by the $PU$-loop method is the local wave speed at the site of measurement of $P$ and $U$. Because $c$ varies with distance along an artery, due to taper or changes in the distensibility, and from vessel to vessel across bifurcations, the calculated value of $c$ will be different from $c$ determined from a transit time measurement which corresponds to a weighted average of $c$ over the distance between measurement sites. The value of a local measure of $c$, and hence distensibility, is shown by the results for the main pulmonary artery seen in Fig. 3. Because the main pulmonary artery in humans branches after only 3–4 cm, it is virtually impossible to use a wave travel time to determine wave speed.

The separation of forward and backward waves depends only upon the density of blood, which varies only minimally, and the local wave speed, which is discussed above. In the absence of large backward waves, as is commonly the case in the normal circulation,

the net wave intensity, $dI = dP\,dU$, is very similar to the forward wave intensity, $dI_+ = dP_+\,dU_+$, and most of the information about the waves can be determined from the magnitude and sign of $dI$. This is the case shown in Fig. 6(a) for the ascending aorta of the dog under control conditions where $dI$ is very similar to $dI_+$ in early and late systole and to $dI_-$ in middle systole. The initial positive peak of $dI$ represents the forward compression wave generated by the initial contraction of the left ventricle. This is followed during mid-systole by a rather small but broad negative peak of $dI$. The small magnitude of $dI$ during this time indicates that the reflected waves reaching the ascending aorta, and hence the heart, are normally very small suggesting that the arterial system is well matched for the transmission of forward waves. The broadness of this peak is undoubtedly due to the large variety of distances to the major reflection sites, probably the high resistance peripheral arterioles, in the systemic circulation. At the end of systole there is another positive peak of $dI$ representing a forward expansion wave generated by the ventricle when it ceases to contract (Parker et al., 1988). Little or no wave intensity is seen during diastole.

If there are large reflected waves, as is the case when the aorta is occluded as shown in the top half of Fig. 2, then the net wave intensity can be misleading indicating, for example, zero wave intensity at a time when a large forward wave is cancelled by an equally large backward wave. This is seen in Fig. 6(b) which shows $dI$ and $dI_\pm$ calculated from $P$ and $U$ measured during aortic clamping. Here the large reflected wave indicated by the peak in $dI_-$ arrives back to the ascending aorta while there is still a substantial forward wave generated by the initial ventricular contraction. Here $dI = dI_+ + dI_-$ gives a misleading picture about the timing and the magnitude of the reflected wave which can only be determined from the separated wave intensities. In fact, the second peak of $dI_-$ seen in Fig. 6(b), which we believe is the reflection of the second peak of $dI_+$ from the site of occlusion, would be very easy to miss in the $dI$ curve.

The dashed lines on either side of the curves of $dI_+$ and $dI_-$ in Fig. 6(b) are the separated wave intensities calculated using a value for $c$ which is 20% larger and smaller than the value calculated from the $PU$-loop in Fig. 2. This was done to test the sensitivity of the wave separation calculation to $c$. Since it would be difficult to make a 20% error in the determination of the slope of the linear portion of the $PU$-loop, these results give us a great deal of confidence in the reliability of the separation of the measured $P$ and $U$ into their forward and backward components.

The separated $P_\pm$ and $U_\pm$ waveforms shown in Fig. 7 are calculated by integrating the differential $dP_\pm$ and $dU_\pm$ curves. It is harder to discern the magnitude and timing of the individual waves from these curves but they are useful in indicating their overall effects. Note that if we are interested in the pressure producing performance of the heart it may be better to consider the $P_+$ waveform rather than the $P$ waveform which can include a significant effect from wave reflections.

The $P_\pm$ and $U_\pm$ curves also illustrate a shortcoming of the wave intensity analysis. During diastole there is a regular decrease of pressure which is not due to waves, as evidenced by the absence of any measurable velocity during diastole, but to the Windkessel effect. The result of this on the separation algorithm can be seen in the prediction of unrealistically large, self-cancelling values of $U_+$ and $U_-$ during diastole. Correction of this anomaly will require incorporation of the mechanics of the global properties of the arterial system which give rise to the Windkessel effect with those of the local mechanics which give rise to the wave nature of the flow.

In conclusion, we believe that the $PU$-loop method of determining wave speed is well founded theoretically and easy to implement experimentally. From our experiments, we believe that the wave speeds thus determined are at least as accurate as those determined by other methods and certainly superior to time of flight methods for determining local wave speeds. Because of the direct relationship between the local wave speed and the local distensibility of the artery, the determination of wave speed can be useful in assessing changes in the mechanical properties of arteries with disease or pharmacological intervention. Finally, we have demonstrated that it may be important to separate forward and backward waves in order to assess accurately the timing and magnitude of arterial waves.

## Acknowledgements

We would like to thank Prof. J.V. Tyberg, Cardiovascular Research Group, University of Calgary for encouragement, invaluable advice and the use of the facilities used in the measurement of the dog data. We would like to thank Prof. A. Redington and Dr. P. White, Great Ormond Street Hospital for Sick Children and University College Hospital, London for the pulmonary artery data. We would like to thank Dr. D.G. Gibson for his continued encouragement and support.

## References

Avolio, A.P., Chen, S.G., Wang, R.P., Zhang, C.L., Li, M.F., O'Rourke, M.F., 1983. Effects of aging on changing arterial compliance and left ventricular load in a northern Chinese urban community. Circulation 68, 50–58.

Belinda, H.A., Lucas, C.L., Henry, G.W., Frantz, E.G., Ferriero, J.I., Wilcox, B.R., 1994. Effects of chronically elevated pulmonary

arterial pressure and flow on right ventricular afterload. American Journal of Physiology 267 (Heart Circ. Physiol. 36), H155–H165.

Dujardin, J.-P.L., Stone, D.N., 1981. Characteristic impedance of the proximal aorta determined in the time and frequency domain: a comparison. Medical and Biological Engineering and Computers 19, 565–568.

Dumoulin, C.L., Doorly, D.J., Caro, C.G., 1993. Quantitative measurement of velocity at multiple positions using comb excitation and Fourier velocity encoding. Magnetic Resonance Medicine 29, 44–52.

Khir, A., 1999. The Hemodynamic Effects of Aortic Clamping. Ph.D. Thesis, University of London, London.

Latham, R.D., Westerhof, N., Sipkima, P., Rubal, B.J., Reuderink, P., Murgo, J.P., 1985. Regional wave travel along the human aorta: a study with six simultaneous micromanometric pressures. Circulation Research 72, 1257–1269.

Li, J.K.-J., 1986. Time domain resolution of forward and reflected waves in the aorta. IEEE Transactions and Biomedical Engineering 33, 783–785.

Milnor, W.R., 1989. Hemodynamics, 2nd Edition, Williams and Wilkins, Baltimore. Appendix D.

Nichols, W.W., O'Rourke, M.F., 1990. MacDonald's Blood Flow in Arteries, 3rd Edition, Edward Arnold, London. p. 285.

Parker, K.H., Jones, C.J.H., Dawson, J.R., Gibson, D.G., 1988. What stops the flow of blood from the heart? Heart Vessel 4, 241–245.

Parker, K.H., Jones, C.J.H., 1990. Forward and backward running waves in the arteries: analysis using the method of characteristics. Journal of Biomechanical Engineering 112, 322–326.

Pythoud, F., Stergiopulos, N., Meister, J.-J., 1996. Separation of arterial pressure wave into their forward and backward running components. Journal of Biomechanical Engineering 118, 295–301.

Westerhof, N., Sipkema, P., Bos, G.C., van den Elzinga, G., 1972. Forward and backward waves in the arterial system. Cardiovascular Research 6, 648–656.

Young, T., 1809. On the functions of the heart and arteries: the Croonian Lecture. Philosophical Transactions of Royal Society 99, 1–31.